Paper 75

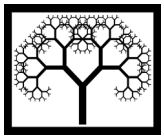

Proceedings of the Eighth International Conference
on Computational Structures Technology,
B.H.V. Topping, G. Montero and R. Montenegro,
(Editors), Civil-Comp Press, Stirlingshire, Scotland.

On the Dynamics of a Duffing Oscillator with an Exponential Non-Viscous Damping Model

D.J. Wagg and S. Adhikari
Faculty of Engineering
University of Bristol, United Kingdom

Abstract

In this paper a Duffing oscillator with non-viscous damping function is considered. The non-viscous damping function is an exponential damping model with a decaying memory property to the damping term of the oscillator. Introducing a non-viscous damping term with a decaying memory kernel means that the governing equation is an integro-differential equation of the Volterra type. Many methods used for the numerical solution of ordinary differential equations (ODE's) can be extended to this type of integro-differential equation. Naturally the solution of the integro-differential equation is more expensive in terms of computational time compared with methods for ODE's. In this system we can exploit the form of exponential damping function to recast the system as a set of three ODE's. Our numerical simulations show that structural changes in the bifurcation diagrams are observed for increasing levels of non-viscous damping parameter. The two cases considered relate to small and large cubic stiffness nonlinearity. The non-viscous damping parameter is found to have an effect on the bifurcation structure in both cases. However, significant changes only occur for large values of non-viscous damping.

Keywords: damping, Duffing, non-viscous, bifurcation.

1 Introduction

Viscous damping is the most common model for modelling of vibration damping. This model, first introduced by Lord Rayleigh [1], assumes that the instantaneous generalized velocities are the only relevant variables that determine damping. Viscous damping models are used widely for their simplicity and mathematical convenience even though the behaviour of real structural materials may not be adequately represented by viscous models. For this reason it is well recognized that in general a

physically realistic model of damping will not be viscous. Damping models in which the dissipative forces depend on any quantity other than the instantaneous generalized velocities are non-viscous damping models. Mathematically, any causal model which makes the energy dissipation functional non-negative is a possible candidate for a non-viscous damping model. Clearly a wide range of choice is possible, either based on the physics of the problem, or by a priori selecting a model and fitting its parameters from experiments. Among various damping models, the 'exponential damping model' is particularly promising and has been used by many authors. With this model the damping force is expressed as

$$f_d(t) = \int_0^t c\,\mu e^{-\mu(t-\tau)}\dot{u}(\tau)\,d\tau. \tag{1}$$

Here c is the viscous damping constant, μ is the relaxation parameter and $u(t)$ is the displacement as a function of time. In the context of viscoelastic materials, the physical basis for exponential models has been well established, see for example [2]. A selected literature review including the justifications for considering exponential damping model may be found in reference [3].

Methods for the analysis of linear single-degree-of-freedom as well as multiple degree-of-freedom systems with damping of the form (1) have been considered by many authors, for example [3–10]. Recently new methods have been proposed [11–13] by which the damping parameters in equation (1) can be obtained from experimental measurements. Studies reported in reference [11] show that the use of viscous damping model when the 'true' damping model is non-viscous can lead to modelling errors. This motivates us to consider non-viscous damping models in non-linear systems. Specifically, in this paper we consider the dynamics of a Duffing oscillator with damping of the form of equation (1).

The Duffing oscillator with viscous damping has been widely studied, and comprehensive reviews of the associated literature can be found in [14–16]. For these type of systems the damping is nearly always assumed to be viscous. One exception is a study of study of a Duffing vibration isolator which has combined Coulomb and viscous damping [17]. In this study the authors demonstrate that the addition of a Coulomb damping term can lead to new dynamical behaviour in the system.

In Section 2 we present the mathematical model of the system, which is then partly nondimensionalised and reduced to an equivalent system of three first order differential equations. The reduced system has six system parameters, of which two relate to the external forcing, two capture the stiffness behaviour, one represents the viscous damping and one the non-viscous damping. Then in Section 3 we show numerical simulations of the system in both phase space, and parameter space. The numerical parameter variation is used to create bifurcation diagrams, in this case using the external forcing frequency as the bifurcation parameter — this allows easy comparison with work on the viscous Duffing system. Structural changes in the bifurcation diagrams are then observed for increasing levels of non-viscous damping parameter. The two cases considered relate to small and large cubic stiffness nonlinearity. The non-viscous damping parameter is found to have an effect on the bifurcation structure in

both cases. However, significant changes only occur for large values of non-viscous damping.

2 Mathematical model

The governing equation for the system can be expressed as

$$m\frac{\mathrm{d}^2x}{\mathrm{d}\hat{t}^2} + c\int_{\hat{\tau}=0}^{\hat{\tau}=\hat{t}} \mu \mathrm{e}^{-\mu(\hat{t}-\hat{\tau})}\frac{\mathrm{d}x}{\mathrm{d}\hat{\tau}}\mathrm{d}\hat{\tau} + \alpha_1 kx + \alpha_2 kx^3 = A\cos(\Omega\hat{t}), \tag{2}$$

where x represents the displacement of mass m, the linear stiffnesses is given by k, coefficients α_j, $j = 1, 2$ represent the form of the stiffness nonlinearity, $\hat{t}$ is time and $\hat{\tau}$ is the integration variable. The viscous damping coefficient is c and the non viscous damping effects are represented by the parameter μ. The forcing amplitude $A = x_0 k$, where x_0 is the equivalent static displacement.

Introducing the nondimensional time variables $t = \hat{t}\omega_n$ and $\tau = \hat{\tau}\omega_n$, where $\omega_n = \sqrt{k/m}$ means that equation 2 can be expressed as

$$\ddot{x} + 2\zeta\int_0^t \frac{\mathrm{e}^{-\frac{1}{\beta}(t-\tau)}}{\beta}\dot{x}d\tau + \alpha_1 x + \alpha_2 x^3 = x_0\cos(\omega t), \tag{3}$$

where $\zeta = c/(2m\omega_n)$, $\beta = \omega_n/\mu$, $\omega = \Omega/\omega_n$ and an overdot represents differentiation with respect to nondimensional time.

We now define the integral term in equation 3 as

$$y = \int_0^t \frac{\mathrm{e}^{-\frac{1}{\beta}(t-\tau)}}{\beta}\dot{x}d\tau. \tag{4}$$

Then by using the Leibniz rule for differentiation of an integral [3] we can write

$$\dot{y} = \frac{1}{\beta}\dot{x} - \frac{1}{\beta}y. \tag{5}$$

We can then write equations 3 and 5 as a set of three first order ordinary differential equations

$$\begin{aligned} \dot{x}_1 &= x_2, \\ \dot{x}_2 &= -2\zeta y - \alpha_1 x_1 - \alpha_2 x_1^3 + x_0\cos(\omega t), \\ \dot{y} &= \frac{1}{\beta}x_2 - \frac{1}{\beta}y, \end{aligned} \tag{6}$$

where all three equations have dimensions of length. We note that if we multiply through the last line of equation 6 by β, then as $\beta \to 0$, $y \to x_2$ and the viscous damping case is obtained.

The parameters $m, c, k, A > 0$ for physically realistic cases. However, the coefficients, α_j $j = 1, 2$ can have positive or negative sign corresponding to the physical case being considered. For example, the case when $\alpha_1 = 1$ and $|\alpha_2| \ll 1$ corresponds to the weakly nonlinear cases of hardening (α_2 positive) or softening (α_2 negative) spring behaviour encountered in a range of mechanical applications. This and other examples will be discussed below.

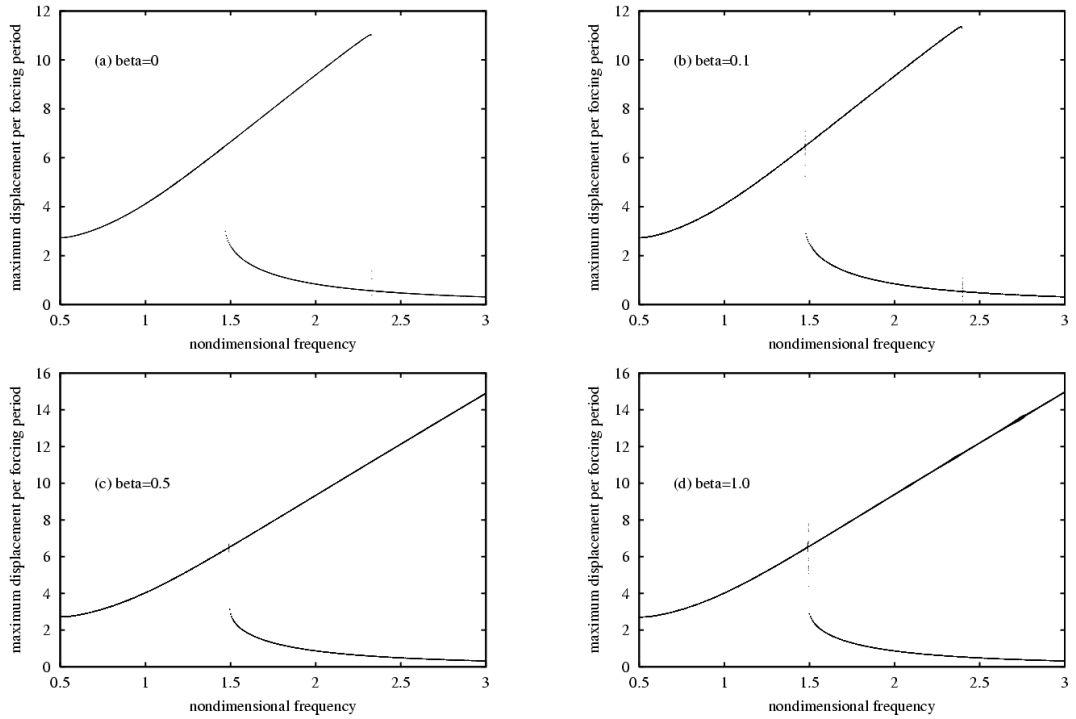

Figure 1: Numerical computation of frequency response plots of the Duffing oscillator with viscous and non-viscous damping. Fixed parameters $x_0 = 2.5$, $\zeta = 0.05$, $\alpha_1 = 1.0$ and $\alpha_2 = 0.05$. (a) Viscous case: $\beta = 0$ (b) $\beta = 0.1$ (c) $\beta = 0.5$ (d) $\beta = 1.0$.

3 Numerical simulations

3.1 Computing solutions

In this section we show numerically computed bifurcation diagrams computed using the "brute force" rather than path following or a continuation approach [18]. Recasting the system as a set of ODE's avoids the need to use computationally expensive approximations to the integro-differential equation of equation 2. The underlying computational method is a 4th order Runge-Kutta integration algorithm, which is fixed step in this case. Using this algorithm and a suitable time step (typically $\Delta = 0.01$ in these simulations), equations 6 can be integrated forward in time.

To create a bifurcation diagram, the simulation is started at the lowest ω value and a number of transient periods are computed (typically 100–200) until a steady state motion is assumed to have been reached. At this point the maximum displacement amplitude per forcing period is recorded for a series of successive steady state periods – typically 20–50. After this ω is increased by a small increment and the process repeated. When the maximum ω is reached the increment is reversed and the process continued back down through the parameter range, finishing at the starting point of minimum ω. We note that this is a simplistic approach which is in no way guaranteed

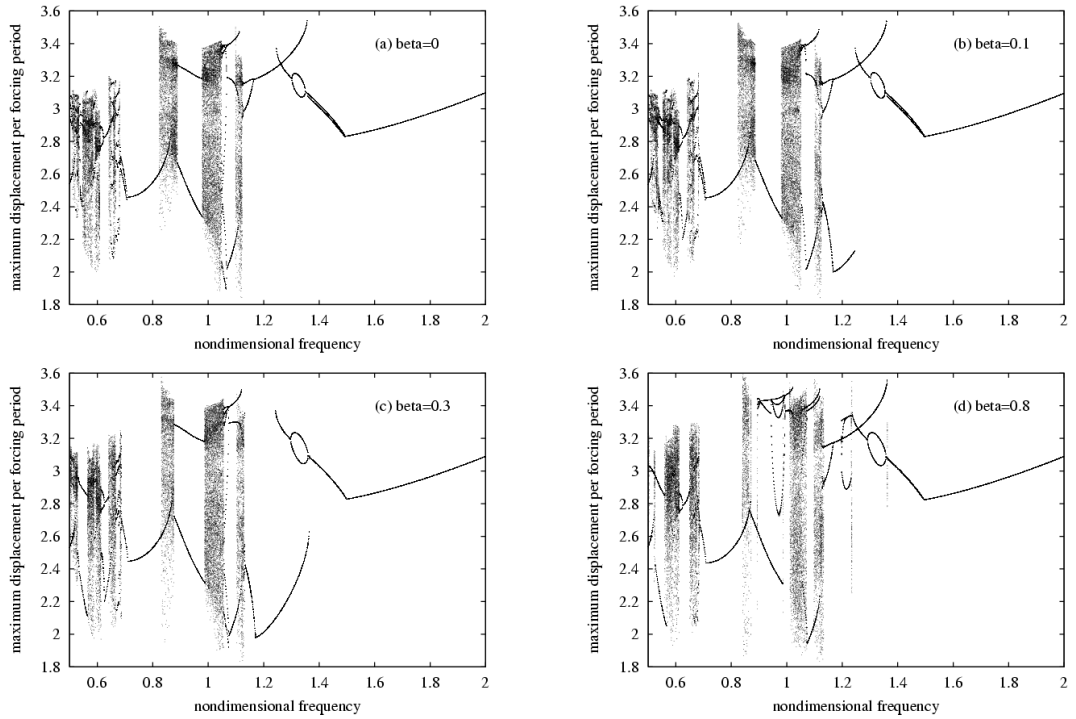

Figure 2: Numerical computation of frequency response plots of the Duffing oscillator with viscous and non-viscous damping. Fixed parameters $x_0 = 7.5$, $\zeta = 0.025$ $\alpha_1 = 0$ and $\alpha_2 = 1.0$. (a) Viscous case: $\beta = 0$ (b) $\beta = 0.1$ (c) $\beta = 0.3$ (d) $\beta = 0.8$.

to locate all possible coexisting solutions — this would require a Monte Carlo (or equivalent) approach. Instead we will focus on the primary resonance behaviour close to $\omega = 1$, and consider what changes occur as the non-viscous damping effects become significant.

3.2 Weak nonlinearity $\alpha_1 = 1$ and $|\alpha_2| \ll 1$

In this subsection we consider the case when $\alpha_1 = 1$, $|\alpha_2| \ll 1$, and $\alpha_2 > 0$. In Figure 1 we show a set of numerically computed frequency response plots for the Duffing oscillator with exponential damping. Figure 1 (a) shows the case when $\beta = 0$, corresponding to viscous damping only. Figure 1 (b)-(d) shows cases of successively increasing β, up to the limit of $\beta = 1$. The result is to extend the resonance peak (in (c) and (d) beyond the limit of the frequency range).

3.3 Strong nonlinearity $\alpha_1 = 0$ and $\alpha_2 = 1$

In the case of a strong nonlinearity, the Duffing system is known to exhibit complex dynamic behaviour including chaos [16]. For these simulations we examine the case when $x_0 = 7.5$, $\zeta = 0.25$, $\alpha_1 = 0$ and $\alpha_2 = 1$. Again we focus our attention on

the region close to $\omega = 1$, where a region of complex dynamical behaviour exists. In Figure 2 we show numerically computed bifurcation diagrams of the system as ω is varied. Figure 2 (a) shows the viscous damping $\beta = 0$ case, and (b)-(d) show cases for increasing β. It is interesting to note that in all cases for values greater than $\omega \approx 1.5$ the period one motion exists (as in the simulations shown in Figure 1). The only effect increasing values of β appears to have on this period one curve is to extend it's height (not shown at this scale) as in the example shown in Figure 1. This is in contrast to the region of complex dynamic behaviour which exists for values of ω less than $\omega \approx 1.5$. Here as β is increased we can observe subtle changes in the dynamics. These changes include subtle movement or *shifts* in the location of the different regions of dynamical behaviour along the ω axis. Changes in the periodicity of solutions can also be observed, although as noted above this numerical approach is not guaranteed to capture all coexisting solutions.

3.4 Comparing dynamics using phase portraits

The bifurcation diagrams shown in figure 2 appear to be qualitatively similar. Changes or shifts in the dynamics as ω is varied are subtle, and in this subsection we plot a selection of phase portraits to compare the changes from direct time series computations. In Figure 3, phase portraits are shown for the viscous ($\beta = 0$) case in comparison with a non-viscous case when $\beta = 0.3$. Then for an arbitrary selection of ω values (selected to highlight different behaviours) we can compare the direct time simulation of the two cases. This shows that there can be qualitative differences as in Figure 3 (a) and (b), where a chaotic response (a) has become a periodic orbit (b) — this is the same for Figure 3 (e) and (f). There can also be quantitative changes as in Figure 3 (c) and (d) where both the responses are chaotic, but the magnitude of the maximum velocity of the chaotic attractor has decreased in the non-viscous case. Structural symmetry changes to the periodic orbits are also possible, as shown by the example in Figure 3 (g) and (h).

4 Conclusions

In this paper we have considered the dynamics of a Duffing oscillator with a non-viscous exponential damping model. This system can be reduced to a set of three ODE's, which can then be simulated using a fixed step, 4th order Runge-Kutta algorithm. Numerical simulations were performed to obtain bifurcation diagrams for the cases of weak and strong stiffness nonlinearity. In both cases, increasing the non-viscous damping parameter leads to subtle changes in the system dynamics. For nonlinear system modelling of mechanical or structural applications, this type of non-viscous damping may give improved accuracy of the simulations when compared to experimental data.

Acknowledgements

The authors would like to acknowledge the support of the Engineering and Physical Sciences Research Council. Both DJW and SA are currently EPSRC Advanced Research Fellows.

References

[1] L. Rayleigh, *Theory of Sound (two volumes)*, Dover Publications, New York, 1945 re-issue, second edition, 1877.

[2] L. Cremer and M. Heckl, *Structure-Borne Sound*, Springer-Verlag Berlin, Germany, second edition, 1973, translated by E. E. Ungar.

[3] N. Wagner and S. Adhikari, "Symmetric state-space formulation for a class of non-viscously damped systems", AIAA Journal, 41(5), 951–956, 2003.

[4] D. J. McTavish and P. C. Hughes, "Modeling of linear viscoelastic space structures", Transactions of ASME, Journal of Vibration and Acoustics, 115, 103–110, 1993.

[5] A. Muravyov and S. G. Hutton, "Closed-form solutions and the eigenvalue problem for vibration of discrete viscoelastic systems", Transactions of ASME, Journal of Applied Mechanics, 64, 684–691, 1997.

[6] A. Muravyov and S. G. Hutton, "Free vibration response characteristics of a simple elasto-hereditary system", Transactions of ASME, Journal of Vibration and Acoustics, 120(2), 628–632, 1998.

[7] J. Woodhouse, "Linear damping models for structural vibration", Journal of Sound and Vibration, 215(3), 547–569, 1998.

[8] S. Adhikari, "Dynamics of non-viscously damped linear systems", ASCE Journal of Engineering Mechanics, 128(3), 328–339, 2002.

[9] S. Adhikari, "Qualitative dynamic characteristics of a non-viscously damped oscillator", Proceedings of the Royal Society of London, Series- A, 461(2059), 2269–2288, 2005.

[10] S. Adhikari, "Dynamic response characteristics of a non-viscously damped oscillator", Transactions of ASME, Journal of Applied Mechanics, 2005, accepted for publication.

[11] S. Adhikari and J. Woodhouse, "Identification of damping: part 1, viscous damping", Journal of Sound and Vibration, 243(1), 43–61, 2001.

[12] S. Adhikari and J. Woodhouse, "Identification of damping: part 2, non-viscous damping", Journal of Sound and Vibration, 243(1), 63–88, 2001.

[13] S. Adhikari and J. Woodhouse, "Quantification of non-viscous damping in discrete linear systems", Journal of Sound and Vibration, 260(3), 499–518, 2003.

[14] J. Guckenheimer and P. Holmes, *Nonlinear oscillations, dynamical systems, and bifurcations of vector fields*, Springer-Verlag: New York, 1983.

[15] F. C. Moon, *Chaotic vibrations: An introduction for applied scientists and engineers*, John Wiley: New York, 1987.

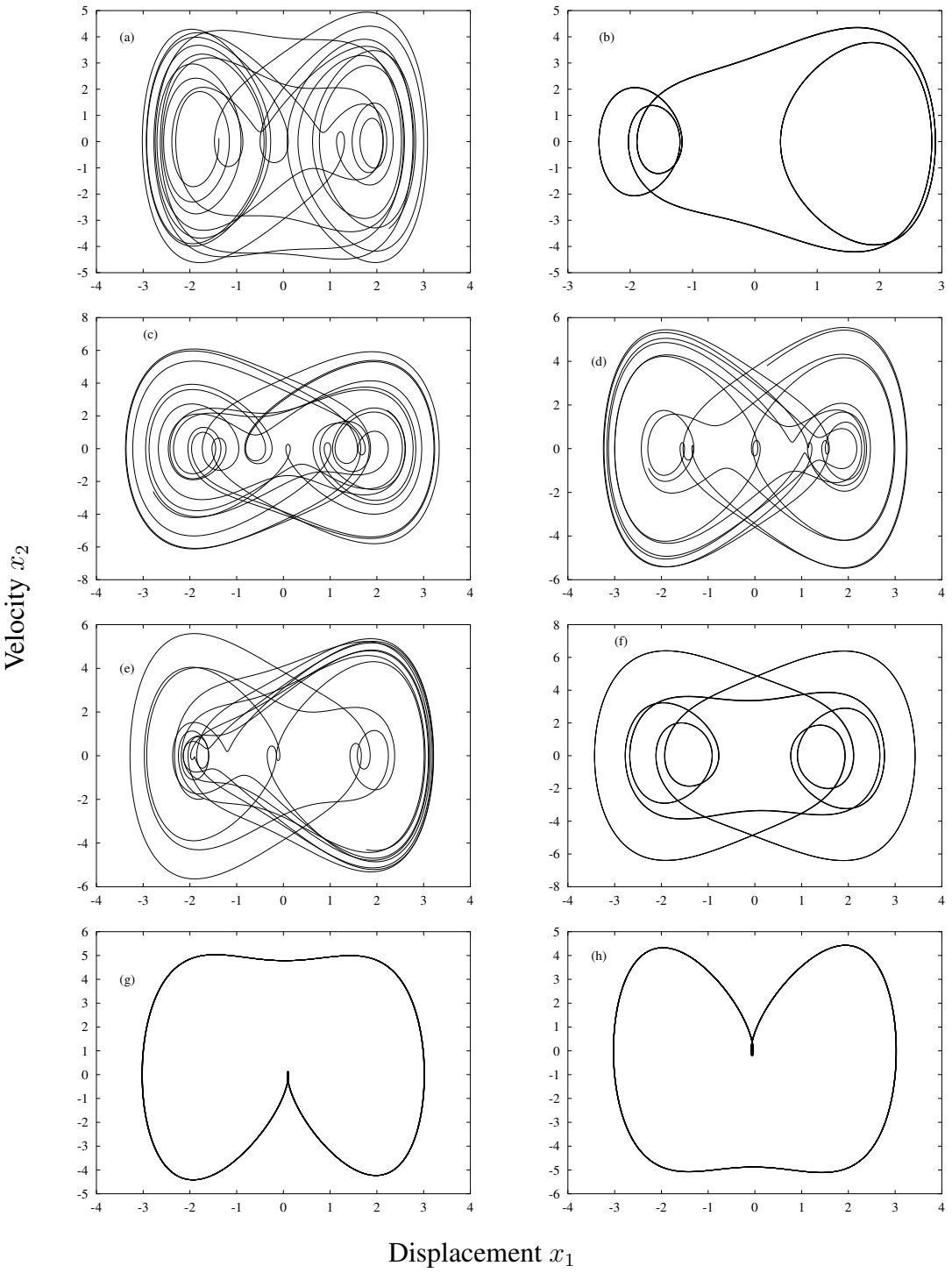

Figure 3: Numerical computation of phase portraits for the Duffing oscillator with viscous and non-viscous damping. Fixed parameters $x_0 = 7.5$, $\zeta = 0.025$ $\alpha_1 = 0$ and $\alpha_2 = 1.0$. Viscous case: $\beta = 0$ is shown in (a) $\omega = 0.65$ (c) $\omega = 1.0$ (e) $\omega = 1.1$ (g) $\omega = 1.4$. Non viscous case $\beta = 0.3$ is shown in (b) $\omega = 0.65$ (d) $\omega = 1.0$ (f) $\omega = 1.1$ (h) $\omega = 1.4$.

[16] J. M. T. Thompson and H. B. Stewart, *Nonlinear dynamics and chaos*, John Wiley: Chichester, 2002.

[17] B. Ravindra and A. K. Mallik, "Hard Duffing type vibration isolator with combined Coulomb and viscous damping", International Journal of Non-linear Mechanics, 28(4), 427–440, 1993.

[18] S. Foale and J. M. T. Thompson, "Geometrical concepts and computational techniques of nonlinear dynamics", Computer Methods For Applications In Mechanical Engineering, 89, 381–394, 1991.